LOX-1 is implicated in oxidized low-density lipoprotein-induced oxidative stress of macrophages in atherosclerosis

HUI-YU YANG[1], YUN-FEI BIAN[1], HUA-PING ZHANG[2], FEN GAO[1], CHUAN-SHI XIAO[3], BIN LIANG[1], JIN LI[1], NA-NA ZHANG[3] and ZHI-MING YANG[1]

[1]Department of Cardiology, The Second Hospital of Shanxi Medical University;
[2]The Scientific Research Laboratory Center, Shanxi Medical University; [3]Department of Cardiology,
The First Hospital of Shanxi Medical University, Taiyuan, Shanxi 030001, P.R. China

Abstract. Induction of oxidative stress has a causal role in atherosclerosis. The aim of the present study was to examine the role of lectin-like oxidized low-density lipoprotein receptor-1 (LOX-1) in oxidized low-density lipoprotein (OxLDL)-induced oxidative stress in atherosclerosis. Small interfering RNA (siRNA) technology was employed to decrease the expression of LOX-1 in mouse RAW264.7 macrophages and the effects of LOX-1 silencing on OxLDL-induced reactive oxygen species (ROS) generation and NADPH oxidase (NOX) expression were investigated. The *in vivo* effects of reducing LOX-1 were also examined in a mouse model (ApoE-/-) of high-fat diet-induced atherosclerosis. Compared with the control cells, OxLDL exposure led to a significant (P<0.05) increase in the intracellular levels of malondialdehyde and ROS and a significant decrease in the activity of superoxide dismutase. Delivery of LOX-1-targeting siRNA significantly (P<0.05) reversed the alterations in oxidative stress parameters induced by OxLDL. LOX-1 silencing downregulated the expression of NOX2, Rac1, p47phox and p22phox and impaired the activation of mitogen-activated protein kinases in OxLDL-treated cells. Adenoviral delivery of LOX-1 siRNA caused a significant increase in the size of the fibrous cap and a decrease in the macrophage content in lesions, compared with the control mice. Western blot analysis demonstrated that the protein expression levels of NOX1, Rac1, p47phox and p22phox in aortic lesions were significantly lower in the LOX-1 siRNA group than in the control group. LOX-1 is implicated in OxLDL-induced oxidative stress of macrophages in atherosclerosis, which in part, involves the regulation of NADPH oxidases.

Correspondence to: Professor Zhi-Ming Yang, Department of Cardiology, The Second Hospital of Shanxi Medical University, 382 Wuyi Road, Taiyuan, Shanxi 030001, P.R. China
E-mail: zhim_yang_013@163.com

Introduction

Atherosclerosis is a leading cause of mortality in developed and developing countries, which is characterized by the development of plaques in arteries that ultimately leads to cardiovascular disease (1). One of the early events of atherogenesis is the formation of foam cells, which are macrophages with ingested oxidized low-density lipoprotein (OxLDL) (2). Compelling evidence indicates that oxidative stress, particularly excessive production of reactive oxygen species (ROS), has a causal role in atherosclerosis (3,4). Lipid oxidation triggered by ROS can amplify foam cell formation through oxLDL formation and uptake. Increased ROS can also promote vasoconstriction, platelet aggregation and adhesion of neutrophils to the endothelium, leading to vascular inflammation and dysfunction in atherosclerosis. The proatherogenic activity of ROS is mediated through activation of numerous signaling pathways, including mitogen-activated protein kinases (MAPKs) (5). p38 MAPK has been implicated in the development of atherosclerosis via promotion of cholesterol ester accumulation in macrophages and foam cell formation (6). Despite extensive studies on the role of ROS in atherosclerosis (3-5), relatively little is known about the molecular mechanisms underlying the regulation of ROS production.

Nicotinamide adenine dinucleotide phosphate (NADPH) oxidases (NOX) are a family of enzymes that use NADPH as a substrate to convert molecular oxygen to ROS (7). In phagocytic cells, NADPH oxidases consist of membrane-associated cytochrome b558 comprising of the catalytic gp91phox (or Nox2) and regulatory p22phox subunits, and cytosolic components, including p47phox, p67phox, p40phox and a small GTPase (Rac1 or Rac2). As a major source of ROS production by vascular cells, NOX enzymes are important in atherosclerosis (8). NOX enzymes have been suggested as important therapeutic targets for the treatment of cardiovascular diseases (9).

Lectin-like oxidized low-density lipoprotein receptor-1 (LOX-1) is the main OxLDL receptor of endothelial cells and is also expressed in macrophages and smooth muscle cells (10). Under physiological conditions, LOX-1 is almost undetectable. However, in response to proatherogenic stimuli (e.g. exposure to OxLDL), LOX-1 is upregulated and can be detected in

atherosclerotic lesions (11). Multiple lines of evidence from animal studies suggest that LOX-1 has a central role in the pathogenesis of atherosclerosis (12,13). Deletion of LOX-1 has been found to attenuate atherogenesis in low-density lipoprotein receptor (LDLR) knockout mice fed a high-cholesterol diet (12). LOX-1 deficiency leads to a reduction in macrophage trafficking in the aorta of LDLR knockout mice (13). There is a close association between LOX-1 expression and ROS generation in human vascular smooth muscle cells (14). However, the role of LOX-1 in OxLDL-induced oxidative stress in macrophages remains to be elucidated.

Therefore, in the present study, small interfering RNA (siRNA) technology was employed to decrease the expression of LOX-1 in macrophages and its effects on OxLDL-induced ROS generation and NOX expression were examined. The *in vivo* effects of reducing LOX-1 were also examined in a mouse model (ApoE-/-) of high-fat diet-induced atherosclerosis.

Materials and methods

Antibodies. Rabbit anti-human LOX-1 polyclonal antibody (cat. no. Ab60178), anti-human Nox2 polyclonal antibody (cat. no. Ab80508), anti-human p22phox polyclonal antibody (cat. no. Ab75941), goat anti-human p47phox polyclonal antibody (cat. no. Ab795), and mouse anti-human Rac1 monoclonal antibody (cat. no. Ab33186) were purchased from Abcam (Cambridge, UK). Rabbit anti-human β-actin polyclonal antibody (cat. no. 4967), anti-human p38 polyclonal antibody (cat. no. 9212), anti-human phosphorylated p38 (cat. no. 9211), rabbit anti-human extracellular signal-regulated protein kinases 1 and 2 (ERK1/2) monoclonal antibody (cat. no. 4965), rabbit anti-human phosphorylated ERK1/2 polyclonal antibody (cat. no. 9101), rabbit anti-human c-Jun NH2-terminal kinase (JNK) polyclonal antibody (cat. no. 9252) and rabbit anti-human phosphorylated JNK monoclonal antibody (cat. no. 4671) were purchased from Cell Signaling Technology, Inc. (Beverly, MA, USA). Rabbit anti-human CD68 polyclonal antibody (cat. no. sc-9139) was purchased from Santa Cruz Biotechnology, Inc. (Santa Cruz, CA, USA). These primary antibodies were diluted 1:1,000 prior to use.

Plasmid and adenovirus construction. Two shRNAs targeting mouse *LOX-1* (GenBank accession no. NM_138648.2) were designed, with target sequences as follows: LOX-1-siRNA1, 5'-GTCAGTGACCCTTATTGTA-3' and LOX-1-siRNA2, 5'-GTGGCCAGTTACTACAAAT-3'. The shRNA oligonucleotides were separately inserted into the pGenesil-1 expression plasmid, which contains the human/mouse U6 promoter and the reporter gene of green fluorescence protein (GFP). The recombinant plasmids were sequenced to confirm the identity of the inserts. LOX-1-shRNA was cloned into an adenoviral shuttle vector and joined with the recombinant adenovirus type 5 (rAd5) vector to construct rAd5-LOX-1-shRNA.

Cell culture, transfection and cell treatment. Mouse RAW264.7 macrophages (ATCC, Manassas, VA, USA) were cultured in Dulbecco's modified Eagle's medium (DMEM; Invitrogen Life Technologies, Carlsbad, CA, USA) containing 10% fetal bovine serum, penicillin (100 U/ml) and streptomycin (100 μg/ml) at 37˚C in a 5% CO_2 incubator.

At 60% confluency, cells were transfected with 1.0 μg LOX-1 shRNA or an empty vector using Lipofectamine 2000 (Invitrogen Life Technologies) and incubated for 24 h at 37˚C. shRNA transfection efficiency was estimated by measuring GFP-positive cells using flow cytometry. The transfection efficiency obtained in the present study was ~72%. LOX-1 mRNA expression was determined using quantitative reverse transcription quantitative polymerase chain reaction (RT-qPCR) analysis, as described below.

Cells were assigned to one of the four treatment groups: Untreated group, no treatment; OxLDL group, treatment with OxLDL; control group, pre-transfection with the empty vector followed by OxLDL exposure and the LOX-1 shRNA group, pre-transfection with LOX-1 shRNA followed by OxLDL exposure. Since LOX-1-siRNA2 demonstrated a higher knockdown efficiency than LOX-1-siRNA1, the former was used in the following experiments. Cells were pre-transfected with the empty vector or LOX-1 shRNA and then exposed to OxLDL (50 mg/l) 24 h after transfection. Following treatment, cells were subjected to oxidative stress and gene expression analyses.

RNA isolation and RT-qPCR analysis. Following treatment, total RNA was extracted from cells using TRIzol reagent (Invitrogen Life Technologies) according to the manufacturer's instructions. Reverse transcription was performed using the AMV First Strand cDNA Synthesis kit (Shanghai Sangon Biological Engineering Technology & Services Co., Ltd., Shanghai, China). qPCR amplification was conducted on an Applied Biosystems StepOnePlus Real-Time PCR System (Applied Biosystems, Foster City, CA, USA). The sequences of the primers and the probe for PCR amplification of LOX-1 were as follows: LOX-1, forward 5'-GCCTCCCAACGAGTTAGAAGAG-3' and reverse 5'-CGGGACGTGGCCATTATATT-3' and 5'-fluorescein-TGGCACTTGTCTGTCACTGGAGCCTGAT-3' (probe). As an internal quantitative control, β-actin was amplified in a parallel reaction with the primers: β-actin, forward 5'-TCAGGTCATCACTATCGGCAAT-3' and reverse 5'-GGATGTCAACGTCACACTTCATG-3', and 5'-fluorescein-TCCAGCCTTCCTTCCTGGGTATGGAATC-3' (probe). All assays were performed in triplicate and the threshold cycle was calculated as described previously (15). The relative LOX-1 mRNA expression level was determined by normalization to β-actin mRNA.

Western blot analysis. Following treatment, cells were resuspended in the lysis buffer containing dithiothreitol and protease inhibitors and lysed on ice. Cell lysates were centrifuged at 12,000 x g for 5 min at 4˚C. Protein content in the supernatants was determined by a BCA protein assay kit (Pierce Biotechnology, Inc., Rockford, IL, USA). Equal quantities of lysate protein were separated by 12% sodium dodecyl sulfate-polyacrylamide gel electrophoresis and transferred onto a polyvinylidene difluoride membrane. Following blocking non-specific sites for 1 h at room temperature with 5% fat-free milk, the membrane was incubated overnight at 4˚C with individual primary antibodies. Following washing, the membrane was incubated with HRP-conjugated secondary
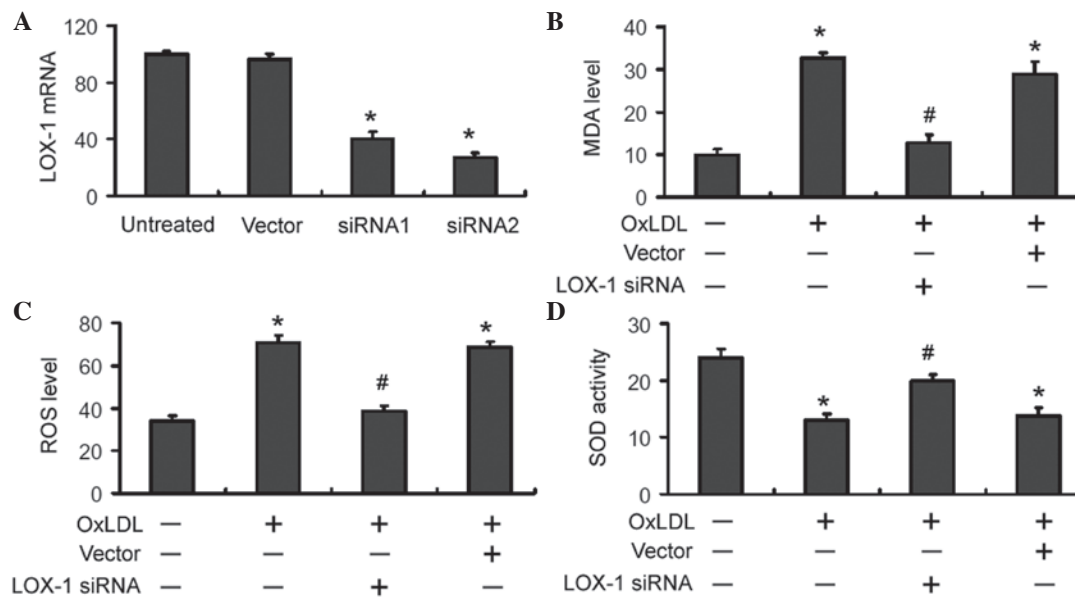
Figure 1. LOX-1 depletion attenuates OxLDL-induced oxidative stress in RAW264.7 macrophages. (A) RAW264.7 macrophages were transiently transfected with LOX-1-siRNA1, LOX-1-siRNA2 or an empty vector. LOX-1 mRNA levels were measured using reverse transcription quantitative polymerase chain reaction. The LOX-1 expression level in untreated cells was arbitrarily assigned as 100%. *P<0.05 vs. untreated cells. (B-D) Cells remained untreated or were exposed to OxLDL with or without pre-transfection with LOX-1-targeting siRNA or the empty vector. (B) MDA and (C) ROS levels and (D) SOD activity were then examined. Data are expressed as the mean ± standard deviation of three independent experiments. *P<0.05 vs. untreated cells; #P<0.05 vs. OxLDL only-treated cells. LOX-1, lectin-like oxidized low-density lipoprotein receptor-1; OxLDL, oxidized low-density lipoprotein; siRNA, small interfering RNA; MDA, malondialdehyde; ROS, reactive oxygen species; SOD, superoxide dismutase.

antibody. Bands were developed by using the diaminobenzidine (DAB) substrate (Sigma-Aldrich, St. Louis, MO, USA). The intensity of signal bands was quantified by densitometry. The relative protein expression level was determined by normalization to β-actin.

Oxidative stress assessment. Following treatment, cells were harvested and intracellular malondialdehyde (MDA) level and superoxide dismutase (SOD) activity were measured using the malondialdehyde colorimetric assay kit and the superoxide dismutase activity assay kit, respectively. (Nanjing Jiancheng Bioengineering Institute, Nanjing, China) according to the manufacturer's instructions.

ROS levels were detected based on the oxidation of 2',7'-dichlorodihydrofluorescein diacetate (DCHF-DA) by peroxide to produce the fluorescent product 2',7'-dichlorofluorescein (DCF). In brief, following treatment, cells were washed and incubated with DCHF-DA (Beyotime Institute of Biotechnology, Haimen, China) for 30 min. Following washing, cells were applied to flow cytometry. The fluorescence of DCF was measured at an excitation wavelength of 488 nm and an emission wavelength of 530 nm.

Animal experiments. In total, 45 ApoE-/- mice (8 weeks old, male) were purchased from Peking University (Beijing, China). Mice were kept on a 12-h light/dark cycle, with food and water freely available. All animals were fed a high-fat diet (1% cholesterol, 10% pork lard and 10% egg yolk) for 5 weeks. The animals were then randomly divided into three groups: Control group (injection of physiological saline), mock group (injection of mock adenovirus) and the LOX-1-siRNA group (injection of the LOX-1-siRNA-expressing adenovirus). The

recombinant adenovirus was administered via tail vein twice with a 10-day interval. Following this treatment, mice were fed the high-fat diet for 4 weeks prior to sacrifice using carbon dioxide anaesthesia. The animal experimental protocol was approved by the Animal Care Committee of Shanxi Medical University (Taiyuan, China).

At the end of the animal experiment, animals were fasted for 12 h and blood samples were obtained from retro-orbital bleeding. The serum levels of total cholesterol, triglycerides and high-density lipoprotein cholesterol were measured using a total cholesterol assay kit, a triglyceride colorimetric assay kit and a high density lipoprotein cholesterol assay kit, respectively. These commercial kits were obtained from Nanjing Jiancheng Bioengineering Institute.

Mice were then perfused via the left ventricle with phosphate-buffered saline followed by 4% paraformaldehyde. The proximal aorta was carefully dissected and fixed overnight in 4% paraformaldehyde prior to embedding in paraffin. Serial 5-μm-thick cryosections were prepared and stained with Movat's pentachrome (Santa Cruz Biotechnology, Inc.) for lesion area quantitation. The plaque area, external elastic membrane area, plaque area/aortic area and fibrous cap area were measured using Image Pro Plus version 6.0 (Media Cybernetics, Bethesda, MD, USA). Additional cryosections from the proximal aorta were stained for macrophages (anti-mouse CD68 antibody), using the standard streptavidin-biotin-peroxidase complex technique. Sections were incubated with biotinylated goat anti-mouse IgG and peroxidase-labeled streptavidin. DAB was used as a substrate chromogen solution for the development of peroxidase activity. Omission of the primary antibody was included as one control to determine staining specificity.
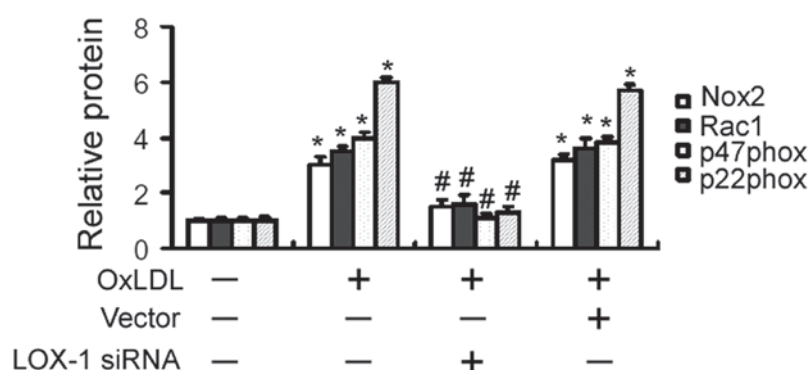
Figure 2. LOX-1 silencing downregulates the expression of Nox2, Rac1, p47phox and p22phox in OxLDL-treated cells. RAW264.7 macrophages remained untreated or were exposed to OxLDL with or without pre-transfection with LOX-1-targeting siRNA or the empty vector and gene expression alterations were measured using western blot analysis. Data are expressed as the mean ± standard deviation of three independent experiments. *P<0.05 vs. untreated cells; #P<0.05 vs. OxLDL only-treated cells. LOX-1, lectin-like oxidized low-density lipoprotein receptor-1; OxLDL, oxidized low-density lipoprotein; siRNA, small interfering RNA.
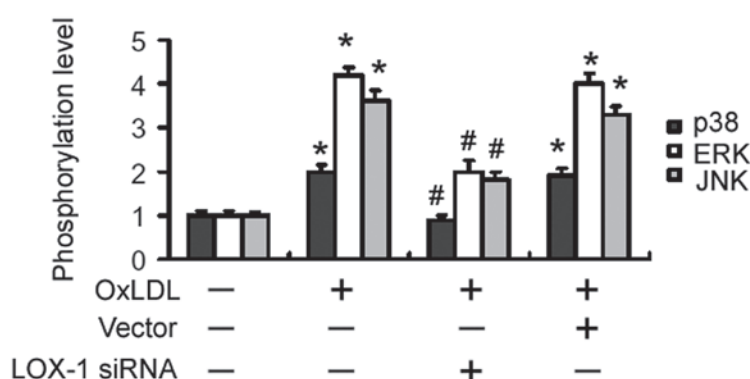

Figure 3. LOX-1 silencing interferes with OxLDL-induced activation of MAPK signaling pathways. RAW264.7 macrophages remained untreated or were exposed to OxLDL with or without pre-transfection with LOX-1-targeting siRNA or the empty vector. The phosphorylation levels of MAPKs were measured using western blot analysis. Data are expressed as the mean ± standard deviation of three independent experiments. *P<0.05 vs. untreated cells; #P<0.05 vs. OxLDL only-treated cells. LOX-1, lectin-like oxidized low-density lipoprotein receptor-1; OxLDL, oxidized low-density lipoprotein; siRNA, small interfering RNA; MAPK, mitogen-activated protein kinase.

Statistical analysis. Data are expressed as the means ± standard deviation. Statistical differences among multiple groups were calculated using one-way analysis of variance followed by Tukey's post hoc test. All statistical calculations were performed using SPSS version 11 software (SPSS, Inc., Chicago, IL, USA). P<0.05 was considered to indicate a statistically significant difference.

Results

LOX-1 depletion attenuates OxLDL-induced oxidative stress in RAW264.7 macrophages. To investigate the role of LOX-1 in OxLDL-induced oxidative stress in macrophages, a LOX-1-siRNA-expressing plasmid was constructed and delivered to RAW264.7 macrophages. As shown in Fig. 1A, transient transfection of LOX-1-targeting siRNA resulted in a significant reduction in the mRNA level of LOX-1 in RAW264.7 macrophages. Compared with untreated cells, OxLDL exposure led to a significant (P<0.05) increase in the intracellular MDA and ROS levels and a significant (P<0.05) decrease in the SOD activity (Fig. 1B-D). Notably, delivery of LOX-1-targeting siRNA significantly (P<0.05) reversed the alterations in oxidative stress parameters induced by OxLDL (Fig. 1B-D).

LOX-1 silencing downregulates the expression of Nox2, Rac1, p47phox and p22phox in OxLDL-treated cells. OxLDL treatment led to a significant elevation in the expression of Nox2, Rac1, p47phox and p22phox, as determined by western blot analysis (Fig. 2). The OxLDL-induced gene expression alterations were significantly inhibited by pre-transfection of LOX-1-targeting siRNA (Fig. 2).

LOX-1 silencing interferes with OxLDL-induced activation of MAPK signaling pathways. Compared with untreated cells, OxLDL-treated cells demonstrated a rapid increase in the phosphorylation levels of p38, JNK and ERK1/2 up to 60 min after treatment, followed by a gradual decrease to basal levels (Fig. 3). When cells were pre-transfected with LOX-1-targeting siRNA, OxLDL-induced activation of MAPKs was significantly impaired (Fig. 3).

Effects of adenoviral delivery of LOX-1 siRNA on body weight, plasma lipid levels and atherosclerotic lesions in ApoE-/- mice. Body weight and plasma lipid levels obtained at the end of the animal experiment were not statistically different among the experimental groups (data not shown). Western blot analysis revealed that adenoviral delivery of LOX-1 siRNA

Table I. Movat pentachrome staining of aortic lesions from ApoE-/- mice.

Group (n=15)	Fibrous cap (μm)	Plaque area (x10³ μm²)	Plaque area/ aortic area (%)
Control	4.78±0.25	189.72±7.21	0.68±0.04
Mock	4.81±0.34	180.04±8.32	0.69±0.03
LOX-1-siRNA	5.41±0.46[a]	169.62±6.14	0.64±0.07

[a]P<0.05 vs. control. LOX-1, lectin-like oxidized low-density lipoprotein receptor-1; siRNA, small interfering RNA.
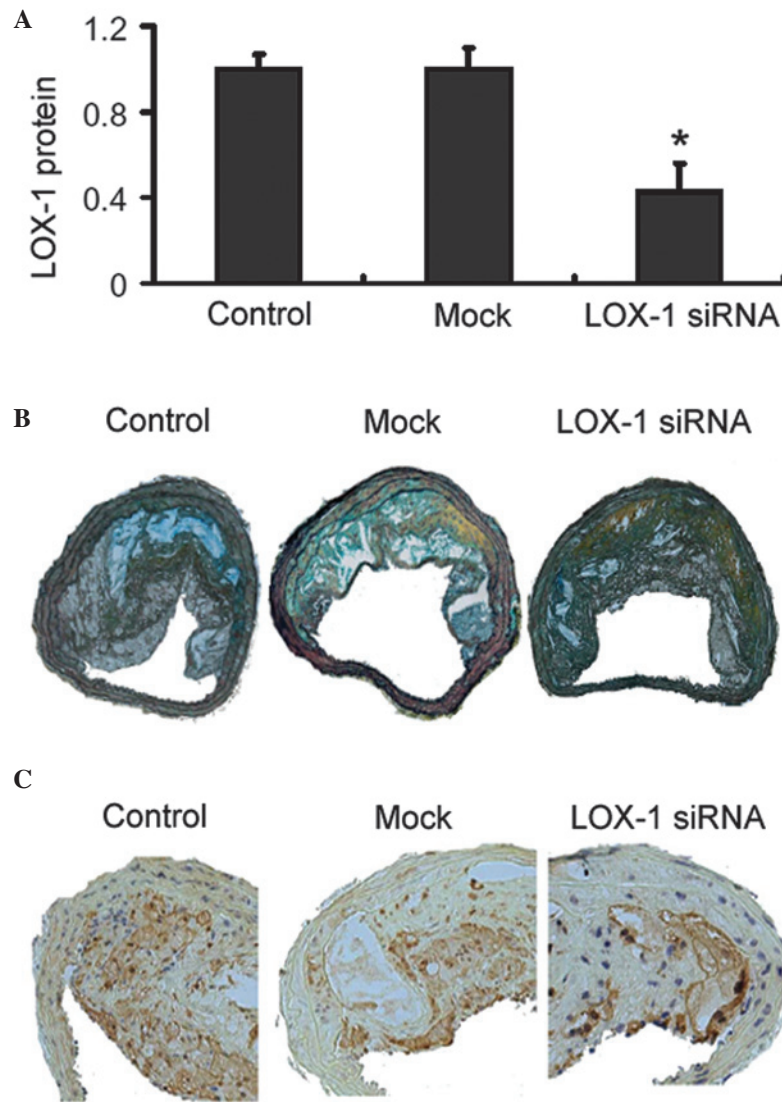

Figure 4. Effects of adenoviral delivery of LOX-1 siRNA on atherosclerotic lesions in ApoE-/- mice fed a high-fat diet. ApoE-/- mice were fed a high-fat diet for 5 weeks and were injected with physiological saline (control), mock adenovirus or an LOX-1-siRNA-expressing adenovirus. Following adenoviral treatment, mice were fed the high-fat diet for 4 weeks prior to sacrifice. (A) Western blot analysis of the LOX-1 expression in the aorta of ApoE-/- mice. Data are expressed as the mean ± standard deviation of three independent experiments. *P<0.05 vs. control. (B) Movat staining revealed that LOX-1 siRNA-treated mice exhibited a marked increase in the size of the fibrous cap, compared with the control mice. (C) Representative photomicrographs of CD68 immunostaining for detection of macrophages in plaques. The delivery of LOX-1 siRNA markedly decreased the macrophage content in lesions, compared with the control group. LOX-1, lectin-like oxidized low-density lipoprotein receptor-1; siRNA, small interfering RNA.

significantly decreased the expression of LOX-1 in the aorta of ApoE-/- mice (Fig. 4A). Movat staining revealed that there were no significant differences in the plaque area, external elastic membrane area and plaque area/aortic area among the animal groups investigated (P>0.05 for each comparison; Fig. 4B and Table I). Notably, LOX-1 siRNA-treated mice exhibited a significant increase in the size of the fibrous cap, compared with the control mice (5.41±0.46 vs. 4.81±0.34,

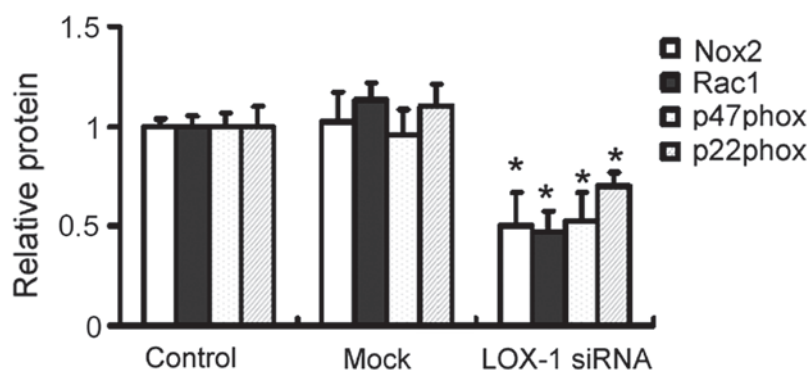Figure 5. Effects of LOX-1 silencing on the expression of Nox2, Rac1, p47phox and p22phox in aortic plaques. ApoE-/- mice were fed a high-fat diet for 5 weeks and were injected with physiological saline (control), mock adenovirus or the LOX-1-siRNA-expressing adenovirus. Following adenoviral treatment, mice were fed the high-fat diet for 4 weeks prior to sacrifice. Western blot analysis of Nox2, Rac1, p47phox and p22phox expression in aortic plaques. Data are expressed as the mean ± standard deviation of three independent experiments. *$P<0.05$ vs. control. LOX-1, lectin-like oxidized low-density lipoprotein receptor-1; siRNA, small interfering RNA; Nox, nicotinamide adenine dinucleotide phosphate oxidase.

$P<0.05$; Fig. 4B and Table I). The delivery of LOX-1 siRNA markedly decreased the macrophage content of lesions, compared with the control group (Fig. 4C).

Effects of LOX-1 silencing on the expression of Nox2, Rac1, p47phox and p22phox in aortic plaques. Western blot analysis demonstrated that the protein expression levels of NOX1, Rac1, p47phox and p22phox in aortic lesions were significantly lower in the LOX-1 siRNA group compared with the control group ($P<0.05$ for each comparison; Fig. 5).

Discussion

Oxidative stress is widely accepted as a critical factor contributing to atherosclerosis (16). A previous study demonstrated that oxygen-free radicals are capable of oxidizing LDL-cholesterol, promoting the formation of foam cells and ultimately leading to the development of atherosclerosis (17). ROS are highly reactive molecules and can affect several biological aspects of atherosclerosis, including endothelial cell, vascular smooth cell and macrophage function and survival as well as lipoprotein metabolism (18). Therefore, it is of significance to determine the mechanisms regulating the production of ROS. Our data revealed that OxLDL exposure induced oxidative stress in macrophages, as evidenced by increased MDA and ROS levels. SOD is a member of the antioxidant family and capable of scavenging cellular ROS, thus representing an important defensive mechanism against oxidative stress (19). It was found that OxLDL treatment led to a significant decrease in the activity of SOD in macrophages, further confirming the induction of oxidative stress. OxLDL-induced macrophage oxidative stress has also been described in a previous study, where OxLDL enhanced ROS formation through the heparin-binding epidermal growth factor-like growth factor-dependent pathway in J774a.1 macrophages (20). LOX-1 is the main OxLDL receptor of endothelial cells (10). Endothelial overexpression of LOX-1 has been found to increase plaque formation and promote atherosclerosis *in vivo* (21). Upregulation of LOX-1 contributes to palmitic acid-induced uptake of OxLDL in macrophage cells (22). The present data indicated the involvement of LOX-1 in OxLDL-induced oxidative stress in macrophages, as

targeting LOX-1 significantly decreased MDA and ROS levels and increased SOD activity in OxLDL-treated macrophages. Since NOX enzymes are a major source of ROS in numerous cell types, the effect of LOX-1 silencing on the expression of NOX enzymes was examined. LOX-1 depletion significantly inhibited the induction of Nox2, Rac1, p47phox and p22phox by OxLDL. Taken together, these results suggest that OxLDL induces macrophage oxidative stress via LOX-1-dependent upregulation of NOX enzymes. To the best of our knowledge, the present study is the first to demonstrate the role of LOX-1 in OxLDL-induced oxidative stress in macrophages. In agreement with the present findings, LOX-1 has been reported to be involved in OxLDL-induced oxidative DNA damage in endothelial cells (23).

Activation of MAPKs is implicated in the development of atherosclerosis (6). It has been documented that MAPK-mediated signaling pathways are involved in *Chlamydia pneumoniae*-induced macrophage-derived foam cell formation (24). Excessive ROS production is responsible for activation of MAPKs in atherosclerosis (5). Pharmacological inhibition of ROS was reported to inactivate p38 MAPK and stress-activated protein kinase signaling, consequently impairing inflammatory responses to lipopolysaccharide in macrophages (25). The present study revealed that accompanying reduction in ROS production, OxLDL-induced phosphorylation of MAPKs was significantly inhibited in LOX-1-depleted macrophages. These findings indicate that prevention of ROS generation due to LOX-1 deficiency adversely affects the activation of intracellular signaling pathways, including MAPKs, which provides a molecular explanation for reduced atherosclerosis in LOX-1-depleted mice (12).

Using a mouse model of high-fat diet-induced atherosclerosis, it was found that LOX-1 depletion led to a significant increase in the size of the fibrous cap. However, the plaque area, external elastic membrane area and plaque area/aortic area were not significantly altered by LOX-1 silencing. Notably, LOX-1 depletion significantly decreased the macrophage content in plaque lesions, coupled with reduced expression of NOX1, Rac1, p47phox and p22phox. These results suggest that LOX-1 silencing protects against atherosclerosis, at least partially, through prevention of oxidative stress via attenuation

of macrophage accumulation and downregulation of NOX enzymes. LOX-1 has been demonstrated to induce macrophage migration in atherosclerosis (13), which provides an explanation for our findings of reduced macrophage accumulation in aortic lesions of LOX-1 siRNA-treated mice.

In conclusion, to the best of our knowledge, the present study provides the first evidence that LOX-1 is required for OxLDL-induced oxidative stress in macrophages, which in part, involves the regulation of NOX enzymes. *In vivo* animal experiments further demonstrate that LOX-1 depletion attenuates high-fat diet-induced atherosclerosis largely through prevention of macrophage accumulation and downregulation of NOX enzymes. These findings suggest that LOX-1 is a promising target for the prevention of atherosclerosis.

Acknowledgements

References

1. Robinson JG and Gidding SS: Curing atherosclerosis should be the next major cardiovascular prevention goal. J Am Coll Cardiol 63: 2779-2785, 2014.
2. Fenyo IM and Gafencu AV: The involvement of the monocytes/macrophages in chronic inflammation associated with atherosclerosis. Immunobiology 218: 1376-1384, 2013.
3. Stocker R and Keaney JF Jr: Role of oxidative modifications in atherosclerosis. Physiol Rev 84: 1381-1478, 2004.
4. Kim YW and Byzova TV: Oxidative stress in angiogenesis and vascular disease. Blood 123: 625-631, 2014.
5. Griendling KK, Sorescu D, Lassègue B and Ushio-Fukai M: Modulation of protein kinase activity and gene expression by reactive oxygen species and their role in vascular physiology and pathophysiology. Arterioscler Thromb Vasc Biol 20: 2175-2183, 2000.
6. Mei S, Gu H, Ward A, Yang X, Guo H, He K, Liu Z and Cao W: p38 mitogen-activated protein kinase (MAPK) promotes cholesterol ester accumulation in macrophages through inhibition of macroautophagy. J Biol Chem 287: 11761-11768, 2012.
7. Bedard K and Krause KH: The NOX family of ROS-generating NADPH oxidases: Physiology and pathophysiology. Physiol Rev 87: 245-313, 2007.
8. Abe J and Woo CH: NADPH oxidase in vascular injury: A new insight about its regulation and role in T cells. Circ Res 104: 147-149, 2009.
9. Drummond GR, Selemidis S, Griendling KK and Sobey CG: Combating oxidative stress in vascular disease: NADPH oxidases as therapeutic targets. Nat Rev Drug Discov 10: 453-471, 2011.
10. Pirillo A, Norata GD and Catapano AL: LOX-1, OxLDL, and atherosclerosis. Mediators Inflamm 2013: 152786, 2013.
11. Gao S and Geng YJ: LOX-1: A male hormone-regulated scavenger receptor for atherosclerosis. Vascul Pharmacol 59: 138-143, 2013.
12. Mehta JL, Sanada N, Hu CP, Chen J, Dandapat A, Sugawara F, Satoh H, Inoue K, Kawase Y, Jishage K, et al: Deletion of LOX-1 reduces atherogenesis in LDLR knockout mice fed high cholesterol diet. Circ Res 100: 1634-1642, 2007.
13. Ding Z, Mizeracki AM, Hu C and Mehta JL: LOX-1 deletion and macrophage trafficking in atherosclerosis. Biochem Biophys Res Commun 440: 210-214, 2013.
14. Dai Y, Mercanti F, Dai D, Wang X, Ding Z, Pothineni NV and Mehta JL: LOX-1, a bridge between GLP-1R and mitochondrial ROS generation in human vascular smooth muscle cells. Biochem Biophys Res Commun 437: 62-66, 2013.
15. Appay V, Bosio A, Lokan S, Wiencek Y, Biervert C, Küsters D, Devevre E, Speiser D, Romero P, Rufer N and Leyvraz S: Sensitive gene expression profiling of human T cell subsets reveals parallel post-thymic differentiation for CD4+ and CD8+ lineages. J Immunol 179: 7406-7414, 2007.
16. Tinkel J, Hassanain H and Khouri SJ: Cardiovascular antioxidant therapy: A review of supplements, pharmacotherapies and mechanisms. Cardiol Rev 20: 77-83, 2012.
17. Prasad K and Kalra J: Experimental atherosclerosis and oxygen free radicals. Angiology 40: 835-843, 1989.
18. Ding Z, Liu S, Wang X, Khaidakov M, Dai Y and Mehta JL: Oxidant stress in mitochondrial DNA damage, autophagy and inflammation in atherosclerosis. Sci Rep 3: 1077, 2013.
19. Fukai T and Ushio-Fukai M: Superoxide dismutases: Role in redox signaling, vascular function and diseases. Antioxid Redox Signal 15: 1583-1606, 2011.
20. Gao P, Wang XM, Qian DH, Qin ZX, Jin J, Xu Q, Yuan QY, Li XJ and Si LY: Induction of oxidative stress by oxidized LDL via meprinα-activated epidermal growth factor receptor in macrophages. Cardiovasc Res 97: 533-543, 2013.
21. Akhmedov A, Rozenberg I, Paneni F, Camici GG, Shi Y, Doerries C, Sledzinska A, Mocharla P, Breitenstein A, Lohmann C, et al: Endothelial overexpression of LOX-1 increases plaque formation and promotes atherosclerosis in vivo. Eur Heart J 35: 2839-2848, 2014.
22. Ishiyama J, Taguchi R, Yamamoto A and Murakami K: Palmitic acid enhances lectin-like oxidized LDL receptor (LOX-1) expression and promotes uptake of oxidized LDL in macrophage cells. Atherosclerosis 209: 118-124, 2010.
23. Thum T and Borlak J: LOX-1 receptor blockade abrogates oxLDL-induced oxidative DNA damage and prevents activation of the transcriptional repressor Oct-1 in human coronary arterial endothelium. J Biol Chem 283: 19456-19464, 2008.
24. Cheng B, Wu X, Sun S, Wu Q, Mei C, Xu Q, Wu J and He P: MAPK-PPARα/γ signal transduction pathways are involved in *Chlamydia pneumoniae*-induced macrophage-derived foam cell formation. Microb Pathog 69-70: 1-8, 2014.
25. Tumurkhuu G, Koide N, Dagvadorj J, Hassan F, Islam S, Naiki Y, Mori I, Yoshida T and Yokochi T: MnTBAP, a synthetic metalloporphyrin, inhibits production of tumor necrosis factor-alpha in lipopolysaccharide-stimulated RAW 264.7 macrophages cells via inhibiting oxidative stress-mediating p38 and SAPK/JNK signaling. FEMS Immunol Med Microbiol 49: 304-311, 2007.